Lifetime dependent flux into the lowermost stratosphere for idealized trace gases of surface origin

Mark Holzer[1,2] and Lorenzo M. Polvani[3,4]

[1]   The flux of idealized trace gases across the thermal tropopause is quantified as a function of their chemical lifetime using the Model of Atmospheric Transport and Chemistry (MATCH) driven by National Centers for Environmental Prediction (NCEP) reanalyses. The flux is computed in the limit of instant stratospheric chemical loss, and tropospheric chemistry is idealized as decay with a constant lifetime, τ_c. Emissions are idealized as time independent, with either a generic anthropogenic pattern or a uniform ocean source. We find that the globally averaged flux into the stratosphere normalized by surface emissions is ∼1% for $\tau_c = 8$ days and ∼30% for $\tau_c \sim 140$ days, slowly approaching the long-lived limit of balance between stratospheric sinks and surface sources. The qualitative τ_c dependence of the globally averaged flux is captured by a simple one-dimensional model. The flux patterns computed with MATCH for the NCEP reanalyses are insensitive to τ_c and reveal preferred pathways into the stratosphere: The divergent circulation feeding isentropic cross-tropopause transport, storm tracks in the winter hemisphere, and isentropic transport to high latitudes.

1.   Introduction

[2]   The exchange of trace gases between the troposphere and the stratosphere has been of intense interest in atmospheric science. This interest stems in large part from the fact that this exchange influences the structure and maintenance of the ozone layer, which in turn plays a major role in the radiative balance of the climate system and in atmospheric chemistry. Of particular interest are so-called very short lived substances (VSLS) [*Law et al.*, 2007; *Montzka et al.*, 2011], chemically reactive tracers with lifetimes of less than half a year that are typically of anthropogenic or biogenic surface origin. VSLS span a wide spectrum of chemical lifetimes ranging from a few hours (e.g., bromoiodomethane), to a few days (e.g., methyl iodide), to several months (e.g., bromochloromethane). A nonhalogenated short-lived trace gas is carbon monoxide (CO), which also contributes to the chemistry of the lower stratosphere [e.g., *Logan et al.*, 1978; *Tian et al.*, 2010]. VSLS are of interest not only

because many are halogenated gases with significant ozone-depletion potentials (ODPs) [e.g., *Wuebbles et al.*, 2001; *Brioude et al.*, 2010; *Pisso et al.*, 2010] but also because of the crucial interplay between chemical lifetime and transport timescales. Because of the short lifetimes, VSLS are not well mixed in the troposphere and their distribution depends strongly on lifetime. It is the focus of this study to isolate the lifetime dependence of troposphere-to-stratosphere (T→S) exchange from other factors affecting VSLS.

[3]   Many previous studies have addressed various aspects of the transport of VSLS. For example, using both Eulerian and Lagrangian tracers, *Levine et al.* [2007] identify the tropical source regions and the regions of the tropical tropopause layer (TTL) that contribute most to transport into the stratosphere. In particular, these authors note that transport into the extratropical lower stratosphere dominates over direct transport into the overworld, a finding we confirm here using a different approach. *Levine et al.* [2007] quantified the tracer mass fraction that survives in the stratosphere after 4 weeks, using idealized tracers with no decay in the stratosphere and simple first-order decay in the troposphere. *Berthet et al.* [2007] used back trajectories from the stratosphere tracked over ∼30 days without any chemical loss to identify the seasonally varying regions of the boundary layer that "ventilate" the lowermost stratosphere, and to distinguish between transport through the tropical and extratropical tropopause layers. *Aschmann et al.* [2009] used an isentropic Eulerian transport model and idealized bromoform and methyl iodide chemistry to confirm the importance of western Pacific surface sources for efficient transport into the stratosphere. *Pisso et al.* [2010] used Lagrangian trajectories and idealized chemistry to evaluate the dependence of ODPs on

[1]Department of Applied Mathematics, School of Mathematics and Statistics, University of New South Wales, Sydney, New South Wales, Australia.
[2]Also at Department of Applied Physics and Applied Mathematics, Columbia University, New York, New York, USA.
[3]Department of Applied Physics and Applied Mathematics and Department of Earth and Environmental Sciences, Columbia University, New York, New York, USA.
[4]Lamont-Doherty Earth Observatory, Palisades, New York, USA.

Corresponding author: M. Holzer, School of Mathematics and Statistics, University of New South Wales, Sydney, NSW 2052, Australia. (mholzer@unsw.edu.au)

surface emission location and seasonality. Both *Aschmann et al.* [2009] and *Pisso et al.* [2010] demonstrate the importance of deep convection for rapid access to the stratosphere, and *Gettelman et al.* [2009] use a one-dimensional transport model with a simple convective scheme to show that convection is important in controlling the vertical profiles of VSLS in the TTL. For a suite of VSLS, *Brioude et al.* [2010] compute the mass fraction that reaches the stratosphere and the associated ODPs, segregated geographically and seasonally. These authors combined a sophisticated Lagrangian transport model with a realistic representation of OH oxidization, photolysis, and wet removal of dissociation products.

[4] In this paper we focus on the lifetime dependence of the flux across the tropopause for idealized tracers with prescribed surface sources. We wish to isolate the effect of the interaction between finite chemical lifetime and transport on the rate with which tracers are delivered to the stratosphere: we do not attempt to model realistic VSLS and their decay products or ODPs, but instead focus on transport. We diagnose the flux of trace gases across the thermal tropopause in terms of their one-way T→S flux. This one-way flux is the flux due to the first cross-tropopause passage of the tracer, which is also the total cross-tropopause flux in the limiting case where the tracer cannot return from the stratosphere because it is efficiently destroyed there. This very simple idealization of stratospheric chemistry is consistent with the expectation of complete dissociation of halogenated VSLS on entry in the stratosphere [*Brioude et al.*, 2010]. Alternatively, one may view the one-way flux as the flux of troposphere-labeled tracer that has its tropospheric identity zeroed on entry into the stratosphere. The simplicity of this stratospheric tracer boundary condition, and the numerical robustness with which the resulting one-way T→S flux can be computed [e.g., *Orbe et al.*, 2012], are the main reasons we choose to focus on the one-way flux. It is worth pointing out that this one-way flux does not suffer from the singularity highlighted by *Hall and Holzer* [2003] because it takes a finite time for surface tracers to reach the stratosphere. One expects the one-way flux to increase with lifetime until stratospheric loss is the only available sink to balance the surface sources, but the detailed dependence of the one-way T→S flux on chemical lifetime has, to the best of our knowledge, not been isolated as a diagnostic of tropospheric transport and cross-tropopause exchange.

[5] In this study, tropospheric chemistry is idealized as a simple loss rate proportional to mixing ratio with a constant chemical lifetime that is independent of time and location, which is a commonly employed approximation [e.g., *Levine et al.*, 2007; *Gettelman et al.*; 2009]. Because our focus here is on transport, we do not track degradation products into the stratosphere, although this is crucial for the purposes of computing ODPs [e.g., *Brioude et al.*, 2010], which are not considered here. For the same reasons, we ignore spatial and temporal variations of the chemical lifetime, which differ among specific chemical species [e.g., *Liang et al.*, 2010; *Hossaini et al.*, 2010] as well as wet and dry deposition processes, which would be important for particular species. Given the idealized nature of our study and the considerable uncertainty in the oceanic emissions of VSLS [e.g., *Quack and Wallace*, 2003; *Butler et al.*, 2007; *Palmer and Reason*, 2009], which likely differ from species to species and are necessarily idealized even in studies that aim for maximum

realism [e.g., *Kerkweg et al.*, 2008], we only consider two time independent idealized emission patterns for both biogenic and anthropogenic sources. We find that, remarkably, the T→S flux of VSLS is only weakly dependent on the emission pattern.

[6] For infinite lifetime, it is clear that the steady state one-way flux into the stratosphere must match the surface source of the trace species, while for zero lifetime, the flux into the stratosphere must be zero. The key questions for this study are thus:

[7] 1. How does the globally averaged flux into the stratosphere depend on chemical lifetime, τ_c, for finite τ_c?

[8] 2. What are the spatial patterns of the T→S flux, and how do they depend on τ_c, given idealized surface emissions?

[9] We emphasize that it is not our goal to simulate any specific trace-gas species or VSLS. Instead, we ask the more general question of how trace gases are transported from the surface to the stratosphere as a function of chemical lifetime. Hence, we focus on highly idealized chemical sources and sinks to elucidate the interplay between transport timescales and chemical lifetimes in controlling T→S fluxes.

2. Methods

2.1. Idealized Tropospheric Chemistry

[10] The mixing ratio χ of each of our chemical tracers obeys

$$\frac{\partial \chi}{\partial t} + \mathcal{T}[\chi] = -\frac{\chi}{\tau_c} \ , \tag{1}$$

where $\mathcal{T}$ is the linear advective-diffusive transport operator, and τ_c is the constant chemical lifetime. Equation (1) holds in the interior of the troposphere and is subject to the boundary conditions of specified emission fluxes at the surface, and zero mixing ratio in the stratosphere. At the surface, we specify a time-independent mass flux $f_s(x, y)$ with global average $\langle f_s \rangle = f_0$. The boundary condition $\chi = 0$ above the thermal tropopause ensures zero return flux from the stratosphere back into the troposphere. The tropopause is located using the standard lapse-rate based WMO definition [*World Meteorological Organization*, 1957]. The resulting statistically cyclostationary flux $f(x, y, t)$ into the lower stratosphere is the focus of this study.

[11] To solve (1) we use MATCH (Model of Atmospheric Transport and Chemistry) driven by NCEP (National Centers for Environmental Prediction) reanalysis data. MATCH is a three-dimensional global model developed by *Rasch et al.* [1997] that uses the mass-conserving SPITFIRE (Split Implementation of Transport using Flux Integral Representation) flux algorithm [*Rasch and Lawrence*, 1998]. We drive MATCH with T62 NCEP reanalyses [*Kistler et al.*, 2001] on a 94 × 192 Gaussian grid (∼1.9° × 1.9°) with 28 hybrid levels. A nonlocal scheme determines the boundary-layer height below which a profile of vertical diffusion coefficients is prescribed, and convection is parameterized by combining a local diffusive scheme [*Hack*, 1994] with a nonlocal penetrative scheme [*Zhang and McFarlane*, 1995].

[12] For $\tau_c < 1$ day, we find that the T→S flux of our idealized tracers is very small, with global averages normalized by the surface source of less than 5×10^{-4}. We therefore examined the approximately exponentially increasing set of lifetimes $\tau_c = 1, 2, 3, 5, 8, 13, 21, 34, 55, 89, 144$ days,

Uniform Ocean Emission Pattern

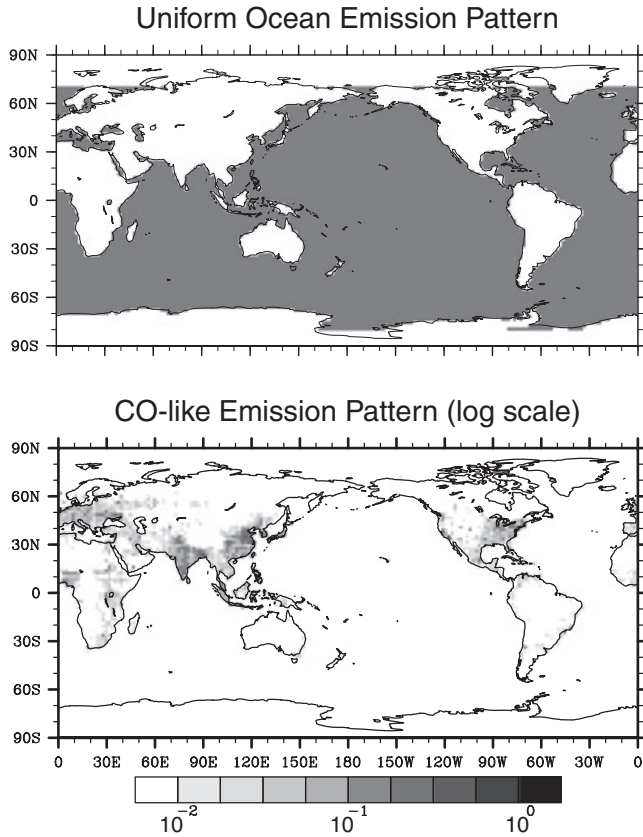## CO-like Emission Pattern (log scale)

Figure 1. The ocean and CO-like surface emission patterns used. Note that the magnitude of the emissions (physically a mass/area/time) is not relevant here because we are interested in the cross-tropopause flux normalized by the globally averaged surface emission flux.

and an additional infinite-lifetime tracer as a check on the numerics. The T→S flux is diagnosed after a spin-up of 22 months when the finite-τ_c tracers have reached a statistically stationary state. We analyze seasonal averages for December, January, and February (DJF) and June, July, and August (JJA), further ensemble averaged over 5 years (2002/2003–2006/2007 for DJF and 2003–2007 for JJA).

2.2. Idealized Surface Emissions

[13] Figure 1 shows the two surface emission patterns used. The uniform ocean source between 80°S and 70°N is relevant for biogenic halogenated species. The actual source pattern for any given oceanic species will likely have considerable spatial and temporal structure [e.g., *Quack and Wallace*, 2003; *Butler et al.*, 2007; *Kerkweg et al.*, 2008; *Palmer and Reason*, 2009], but in the absence of any detailed data with global coverage for each species of the chemical lifetimes considered, and more importantly to focus on lifetime dependence without changing other variables, we simply choose a uniform ocean pattern with the polar regions excluded. The second pattern is that of the normalized EDGAR (Emission Database for Global Atmospheric Research) 2000 anthropogenic CO emissions [*Olivier et al.*, 2005] coarse-grained to the MATCH grid. This pattern is representative of most anthropogenic emissions, which tend to be highly localized. While the patterns

of specific anthropogenic VSLS will differ in detail, one such pattern suffices at the level of idealization considered. Indeed having the same pattern for all species is desirable to cleanly isolate the lifetime dependence of the T→S one-way flux. Note that only the pattern of the emission matters here, because all diagnostics of interest can and will be normalized by the globally integrated emissions.

3. A Simple Model

[14] Before examining the MATCH/NCEP results, it is useful to consider a highly simplified one-dimensional (1-D) analytical model that illustrates the qualitative dependence of the T→S flux on chemical lifetime. For a purely diffusive atmosphere with constant diffusivity κ and no horizontal variations, the transport-operator term of (1) becomes $\mathcal{T}[\chi] = -\rho^{-1}\partial_z(\rho\kappa\partial_z\chi)$, where ρ is the density of air. We prescribe an exponentially decaying density $\rho(z) = \rho_0\exp(-z/H)$ with constant scale height H, and for simplicity, we assume that the tropopause is located at $z = H$. One could introduce a separate tropopause height H_T as an additional parameter, but we intend to use this simple model only for qualitative purposes and therefore chose $H_T = H$. The tracer mass flux into the tropopause at $z = H$, where zero mixing ratio is enforced, is given by $f = -\rho(H)\kappa\partial_z\chi|_{z=H}$. From the steady state solution of (1), one obtains

$$f(\widehat{\tau}_c)/f_0 = e^{-1/2}\,\frac{2s}{2s\cosh(s) - \sinh(s)}\quad,\qquad s \equiv \sqrt{\frac{1}{4} + \frac{1}{\widehat{\tau}_c}}\quad. \quad (2)$$

In (2), we have eliminated explicit dependence on the (unknown) diffusivity by using nondimensional variables: $\widehat{\tau}_c \equiv \tau_c\kappa/H^2$ is the chemical lifetime nondimensionalized with the diffusive timescale H^2/κ.

[15] Figure 2a shows $f(\widehat{\tau}_c)$ given by (2). Note that the approach to the asymptote of $f/f_0 = 1$ takes many (order 10) diffusive timescales H^2/κ. We shall see below that the real troposphere, as approximated by NCEP reanalysis together with MATCH's subgrid parameterizations, similarly approaches the $\tau_c \to \infty$ limit slowly. With $H_T > H$, the approach to the $\tau_c \to \infty$ limit would be yet slower, while with $H_T < H$, the approach would be faster.

[16] Fits of the analytic flux curves (2) to the MATCH simulations show that, as expected, the simple 1-D diffusion model does not capture the short-τ_c asymptotic behavior of the transport accurately. Least-squares fits, with equal weights assigned to the values of τ_c analyzed, show that the analytical curve goes to zero faster as $\tau_c \to 0$ than the simulations do. The episodic fast coherent transport in convective updrafts and in warm conveyor belts cannot be captured by our simple Fickian diffusion model (1). With a nominal scale height of 8 km, the best fits are achieved for effective (vertical) diffusivities of about 2 m^2/s, although given its obvious limitations, we provide the simple 1-D model primarily to demonstrate the very slow convergence to the $\tau_c \to \infty$ limit.

4. Results

[17] Figure 2b shows the MATCH/NCEP-computed, globally averaged flux into the stratosphere, $\langle f \rangle$, as a function of τ_c in DJF and JJA and for both source cases.
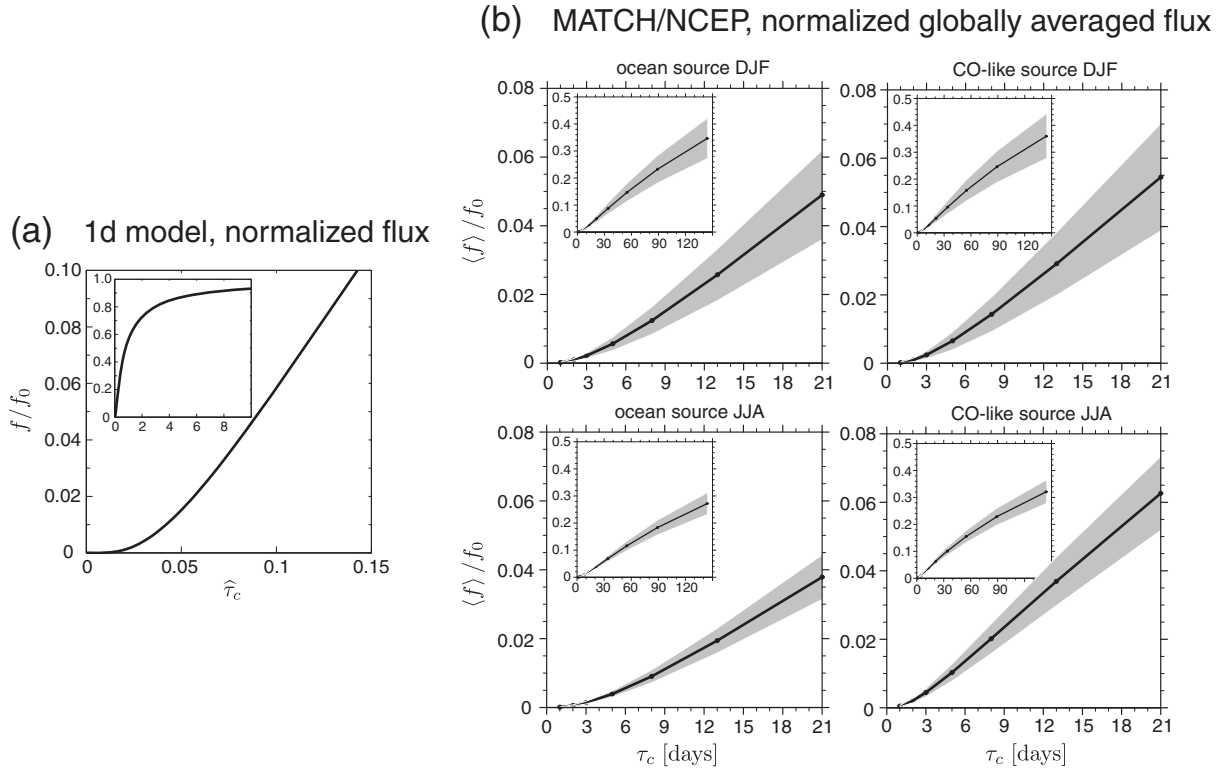
Figure 2. (a) The steady state flux f into the stratosphere, normalized by the surface source f_0, for a 1-D constant-coefficient diffusive atmosphere. The main curve shows f/f_0 for short nondimensionalized chemical lifetimes $\widehat{\tau}_c \equiv \tau_c \kappa / H^2$, and the inset shows f/f_0 for much longer $\widehat{\tau}_c$ to highlight the asymptotic approach to $f/f_0 = 1$. (b) The MATCH/NCEP results for the globally, seasonally, and ensemble-averaged flux $\langle f \rangle$ into the stratosphere normalized by the globally averaged surface source flux f_0. Both source cases are shown for DJF and JJA. The main panels show $\langle f \rangle / f_0$ for $\tau_c \leq 21$ days, while the insets show $\langle f \rangle / f_0$ for all lifetimes studied. The shading indicates $\pm$ one standard deviation of the day-to-day variability.

Quantitatively, the globally averaged T→S flux for $\tau_c = 8$ days is about 1% of the source for the ocean pattern and roughly twice as large for the CO pattern in JJA. The globally averaged T→S flux decreases rapidly with decreasing τ_c and falls below $5 \times 10^{-4} f_0$ for $\tau_c < 1$ day. The $\tau_c \to \infty$ limit of balance between stratospheric sinks and surface sources is approached slowly: For $\tau_c = 144$ days, the T→S flux is still only about 35% of the global source for both emission cases during DJF, and 27% of the ocean source and 32% of the CO-like source during JJA. Remarkably, the dependence of $\langle f \rangle / f_0$ on τ_c is qualitatively similar to that of the simple analytical 1-D model (Figure 2a), with similar very slow convergence to the $\tau_c \to \infty$ limit.

[18] The standard deviation of the day-to-day variability in $\langle f \rangle / f_0$ is about twice as large in DJF ($\pm \sim 0.08$ for $\tau_c = 144$ days) as in JJA. Given that the main entry points into the stratosphere lie in the Northern Hemisphere (NH) in DJF, and in the Southern Hemisphere (SH) in JJA (see below), this seasonality in the flux variability is consistent with the recent results of *Son et al.* [2011] that show greater tropopause variability in the NH during DJF than in the SH during JJA.

[19] Figure 3 shows maps of the seasonally and ensemble-averaged flux across the thermal tropopause for $\tau_c = 5$ and 144 days. For lifetimes between these two values, the flux patterns are intermediate. In DJF, the dominant qualitative features of the flux patterns are very similar regardless of lifetime and emission pattern (including $2 \leq \tau_c < 5$ days, not shown), excepting the flux at high latitudes (e.g., over Antarctica) which grows with τ_c relative to the rest of the pattern. In JJA for the ocean source, the flux patterns are similarly insensitive to τ_c. In JJA for the CO-like source, the flux patterns in the NH are only weakly dependent on τ_c, but they continue to change with τ_c in the SH, where there are almost no anthropogenic sources. The bulk of anthropogenic tracer in the SH troposphere is supplied by interhemispheric transport. Remarkably, even in JJA, a lifetime of $\tau_c = 144$ days is sufficient for the two source cases to have T→S fluxes with broadly similar features in the tropics and subtropics. For $\tau_c < 2$ days (not shown), the flux patterns do depend on the details of the emissions, but less than 0.2% of the tracer reaches the tropopause.

[20] The overall insensitivity of the flux features to both chemical lifetime and source pattern underlines that the lower stratosphere is reached via preferred pathways and cross-tropopause conduits that are visible in Figure 3: In the winter hemisphere, there is a signature of the storm tracks of midlatitude cyclones whose warm conveyor belts rapidly move air aloft [e.g., *Stohl*, 2001; *Sprenger and Wernli*, 2003; *Berthet et al.*, 2007]. This is particularly visible for the CO-like source over the North Pacific and for the ocean source in the SH between 40°S and 60°S. There is also enhanced

Normalized Flux into the Stratosphere
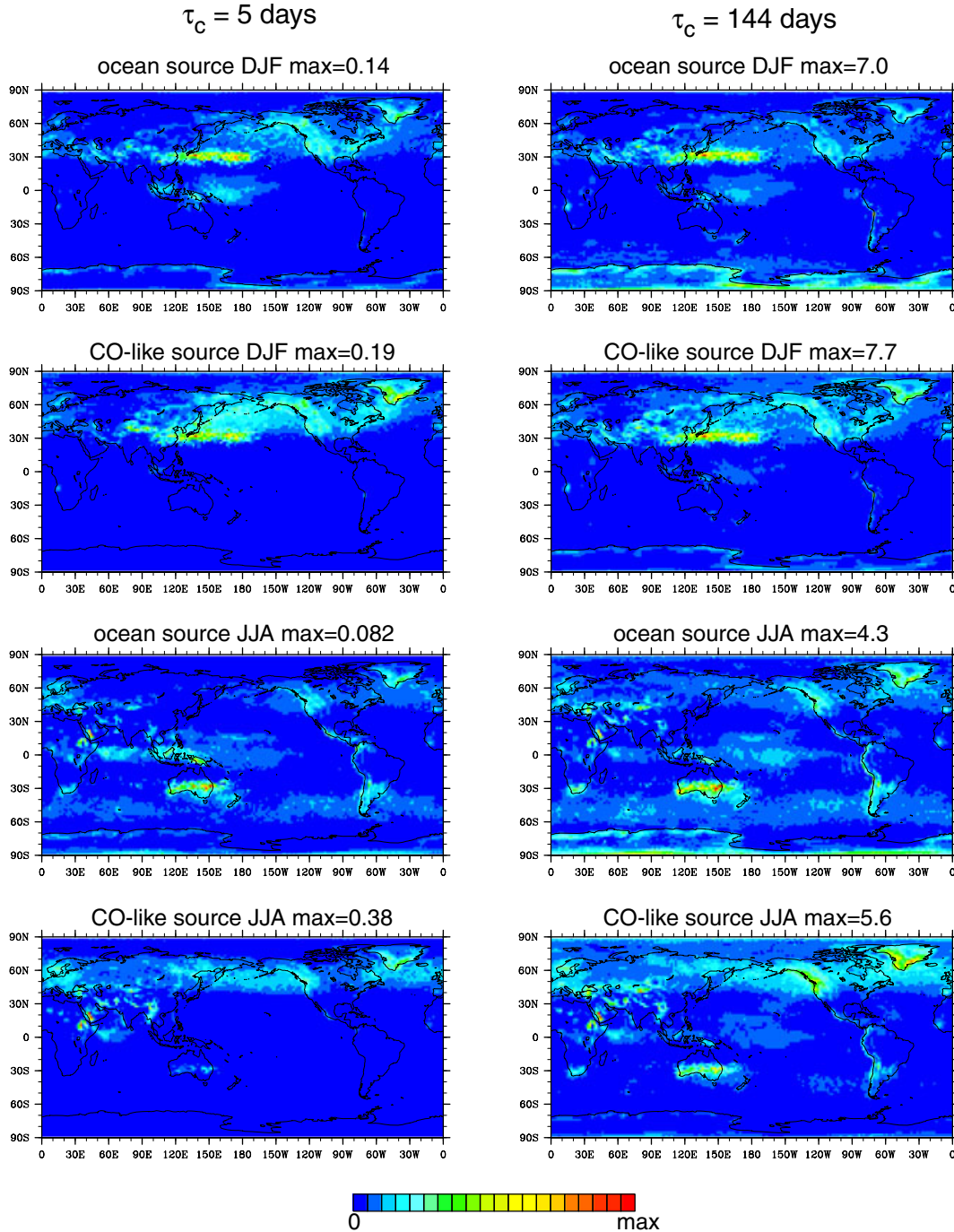
τ_c = 5 days

τ_c = 144 days

Figure 3. The seasonally and ensemble-averaged flux into the stratosphere for τ_c = 5 and 144 days. Both source cases are shown for DJF and JJA. The flux has been normalized by the globally averaged surface source flux, as are all diagnostics computed in this study. The maximum value of the color scale is indicated in the title of each plot.

T→S flux over the mountainous terrain of North America, Greenland, and the Andes, possibly associated with orographic lift. High T→S flux over southern Greenland was also diagnosed in the Lagrangian study by *Sprenger and Wernli* [2003]. At longer τ_c, enhanced flux develops over polar latitudes, particularly over Antarctica for the dominantly SH ocean source. The flux at high latitudes is likely associated with isentropic transport that connects the surface to the upper polar troposphere.

[21] Perhaps the most interesting feature visible in Figure 3 is a sharp line of pronounced flux in the winter hemisphere at latitude ~30° extending in longitude from ~100°E–180° in the general vicinity of Indonesia and the Pacific warm pool. The sharp flux line is likely due to tracer
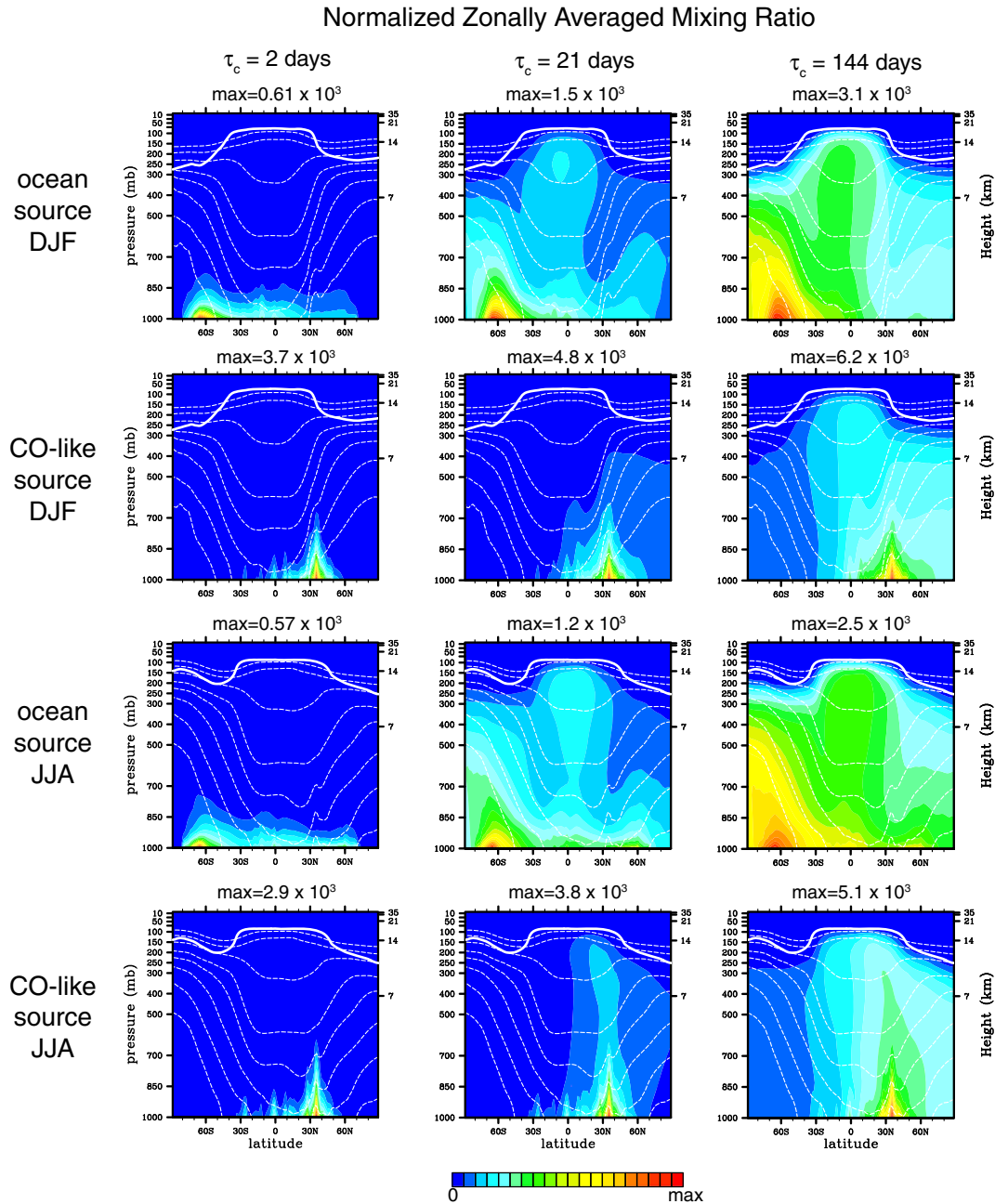
Normalized Zonally Averaged Mixing Ratio

Figure 4. The ensemble, seasonal, and zonal average of the tracer mixing ratio for the DJF and JJA seasons and the chemical lifetimes, τ_c, indicated. Results for both the ocean and CO-like emissions are shown. The zonally averaged mixing ratio has been normalized by its maximum, indicated in the title of each panel in units that correspond to a globally averaged surface source of unity. The dashed contours are zonally averaged isentropes from 280K to 320K in 10K intervals, and from 320K to 380K in 20K intervals, and the solid white line indicates the mean tropopause.

that is transported into the upper tropical troposphere by both deep convection and large-scale low-level convergence. In the upper tropical troposphere, the tracer is then swept by the divergent outflow of the Hadley-Walker circulation toward the winter hemisphere, where the tracer crosses the tropopause isentropically with Rossby waves (clearly visible in animations) in the vicinity of the subtropical jet, creating the sharp line of T→S flux. The 200-hPa divergent winds have a seasonality and spatial pattern [e.g., *Trenberth*

et al., 2000] that is consistent with the appearance of the flux lines in the winter hemisphere and with their longitudinal extent, which roughly coincides with the strongest divergent winds.

[22] This mechanism for producing the flux line in the winter hemisphere is also reflected in the zonally averaged structure of the tracer mixing ratio shown in Figure 4. On the scale of the figure, the panels for $\tau_c = 144$ days and the ocean source shows a tropical tracer "plume" reaching

the upper troposphere with sharp horizontal gradients toward the steeply inclined part of the tropopause in the winter hemisphere. (Such a tropical tracer plume exits also for τ_c = 2 and 21 days but is not visible on the scale of the surface mixing ratio.) These gradients are precisely what one would expect from isentropic cross-tropopause transport at ~30° latitude into a stratosphere where the tracer is instantly removed. Upper-level outflow from tropical tracer plumes toward the winter hemisphere has also been diagnosed in a free-running GCM [*Holzer*, 1999].

[23] It is worth emphasizing that the patterns of preferred entry into the stratosphere visible in Figure 3 do not simply consist of tropical regions with a maximum over the western Pacific and Indonesia, as is commonly seen with Lagrangian trajectory studies of cross-tropopause exchange [e.g., *Fueglistaler et al.*, 2004; *Bonazzola and Haynes*, 2004; *Krüger et al.*, 2008; *Fueglistaler et al.*, 2004]. The reason why our one-way T→S flux patterns are different is that we consider all flux across the tropopause, while the Lagrangian studies typically only select trajectories that connect the troposphere to the overworld (for example by starting back trajectories in the overworld). Thus, while Figure 3 shows a clear signature of the tropical tropopause being crossed over the western Pacific (e.g., the τ_c = 144 day, ocean-source case), the overall pattern of the one-way T→S flux is in fact dominated by the flux lines discussed above where short-lived substances enter the extratropical lower stratosphere (that is, the stratospheric middleworld) isentropically. The dominance of transport into the stratospheric middleworld over transport into the overworld was also noted by *Levine et al.* [2007], who estimated that 95% of the air transported from the TTL into the stratosphere is transported into the stratospheric middleworld, with only about 5% ascending directly into the overworld.

[24] Figure 5 quantifies the τ_c dependence of the T→S flux in terms of the zonally averaged flux $[f]/f_0$. The flux lines associated with isentropic cross-tropopause transport are manifest as the dominant peak at ~30°N in DJF, and the smaller peak at ~30°S in JJA. Figure 5 also quantifies the differences between the two source cases, with the predominantly NH CO-like emissions leading to larger values of $[f]/f_0$ north of ~45°N. The overall amplitude of $[f]$ grows with increasing τ_c in accord with Figure 2, while the patterns of $[f]$ display the weak τ_c dependence seen in Figure 3. Another prominent feature of $[f]$ is a peak at high latitudes that increases with increasing τ_c relative to the rest of the pattern as the polar tropopause becomes isentropically more accessible. While the polar fluxes (mass flow rate per unit area) may be locally important, it must be kept in mind that they pass through only a small area. Area weighting the fluxes (thus converting to a mass/time flow rate) eliminates the high-latitude peaks.
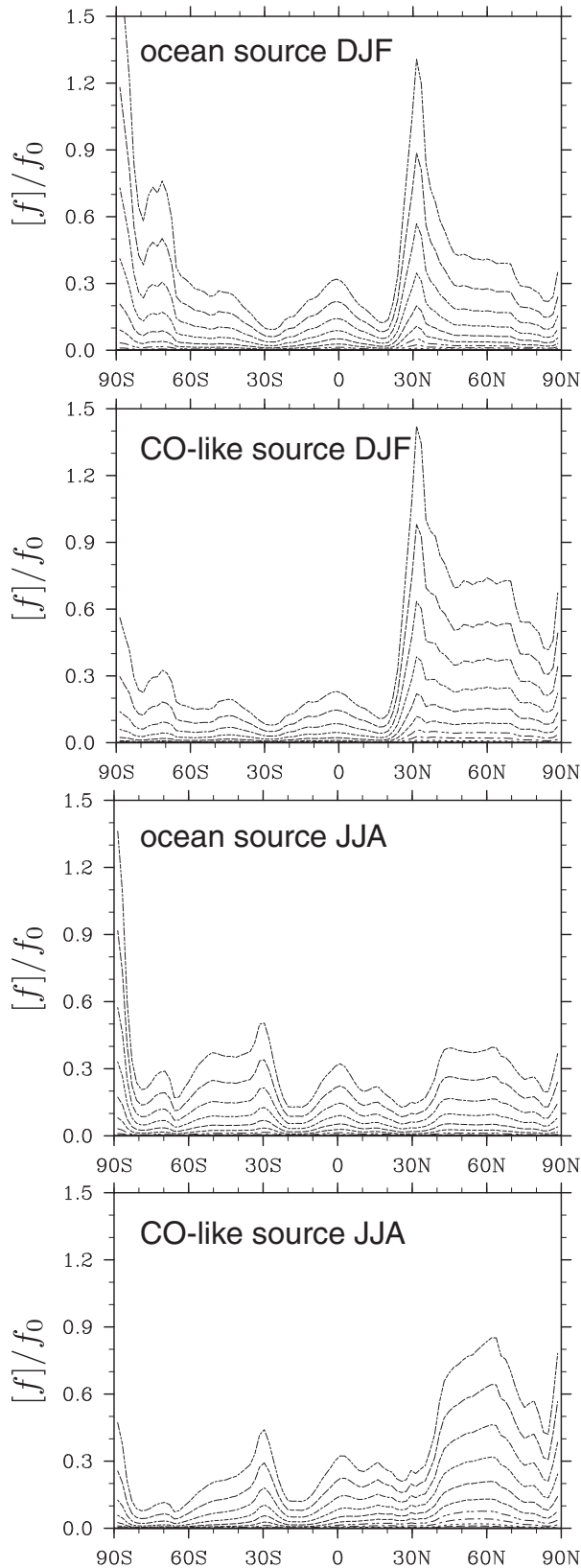
Figure 5. The seasonally and zonally averaged normalized flux into the stratosphere, $[f]/f_0$, for DJF and JJA and both source cases, as indicated. For each panel, the topmost curve corresponds to τ_c = 144 days, the curve below that to τ_c = 89 days, and so on for τ_c = 55, 34, 21, 13, 8, 5, 2, and 1 days.

5. Discussion

[25] We have quantified the one-way flux of idealized trace gases with chemical lifetimes $1 \leq \tau_c \leq 144$ days across the thermal tropopause using MATCH driven by NCEP reanalyses. We acknowledge that both model and

reanalyses have limitations. The MATCH model is subject to possible biases because convection and boundary-layer processes are not resolved by the NCEP data and therefore need to be parameterized. While beyond the scope of our study, it would be useful to repeat our calculations with different convective parameterizations to quantify the sensitivity of the T→S flux to processes not resolved in the NCEP data. This is particularly important in light of the strong transport from the upper tropical troposphere into the lower stratosphere produced by MATCH/NCEP, and the general importance of convection for the transport of short-lived species [e.g., *Aschmann et al.*, 2009; *Gettelman et al.*, 2009; *Pisso et al.*, 2010].

[26] The NCEP reanalysis data has issues of its own: *Pawson and Fiorino* [1998] document some of the NCEP biases by comparing with European Centre for Medium-Range Weather Forecasts (ECMWF) reanalyses (ERA) [*Gibson et al.*, 1997]. A recent analysis of the NCEP biases in surface fluxes is provided by *Decker et al.* [2012]. Although our results would certainly be quantitatively different had we used ERA or some other meteorological driving data, the qualitative character of the lifetime dependence and patterns of the one-way T→S flux would likely be unchanged given that these patterns are organized by the large-scale tropospheric flow, and the fact that MATCH does not rely on the analyzed winds to represent convection but instead uses an updraft ensemble parameterization for deep convection [*Zhang and McFarlane*, 1995]. Improvements from using diabatic heating rates in the upper TTL for advecting Lagrangian particles [e.g., *Krüger et al.*, 2008; *Wohltmann and Rex*, 2008] cannot readily be applied to MATCH and lie beyond the scope of our analysis.

6. Conclusions

[27] The goal of this study has been to quantify how the interplay between chemical lifetime and tropospheric transport controls the T→S flux of short-lived species. By using highly idealized chemistry and emission patterns, we have isolated the lifetime dependent patterns of the one-way T→S flux, thus complementing the many existing studies on the cross-tropopause exchange of VSLS. Our key findings are as follows:

[28] 1. The dependence of the globally averaged flux $\langle f \rangle$ on chemical lifetime τ_c is qualitatively similar to that of a very simple 1-D diffusion model. For tracers with $\tau_c < 1$ day, $\langle f \rangle$ is less than 5×10^{-4} the globally averaged source flux f_0, and for $\tau_c = 8$ days $\langle f \rangle / f_0 \sim 1\%$, the exact value depending on season and emission pattern. The approach to the long-lived limit of $\langle f \rangle = f_0$ is very slow: For lifetimes of about 5 months, roughly two thirds of the tracer is still destroyed ("oxidized") in the troposphere before reaching the lower stratosphere ($\langle f \rangle / f_0 \sim 30\%$ for $\tau_c = 144$ days).

[29] 2. The spatial pattern of the one-way flux into the lower stratosphere is insensitive to both the geographic distribution of the emissions and the chemical lifetime, except for fluxes into the polar regions; these increase with increasing lifetime due to isentropic access to the high-latitude lower stratosphere. The polar fluxes are most pronounced over Antarctica for the predominantly SH ocean source, but because they occur over a small area, they make a negligible contribution to the globally averaged flux.

[30] 3. The T→S flux patterns reveal preferred pathways into the lower stratosphere, suggesting the following three main routes by which tracers of surface origin reach the lower stratosphere: (i) In regions of tropical deep convection and large-scale low-level convergence, ascent into the upper troposphere is followed by upper-level outflow with the dominant Hadley cell, which feeds isentropic transport into the stratospheric middleworld. (ii) Enhanced T→S flux is associated with the winter hemisphere's storm tracks, where warm conveyor belts are the likely mechanism for rapid transport into the lower stratosphere [e.g., *Stohl*, 2001; *Berthet et al.*, 2007]. (iii) For lifetimes greater than a few days, isentropic transport to polar regions becomes locally important.

[31] Our findings are in broad agreement with those of *Levine et al.* [2007], who also find that the lateral transport into the stratospheric middleworld dominates over fluxes through the tropical tropopause into the overworld. Although we use a different methodology and different meteorological data (NCEP versus ECMWF), our findings are in qualitative and approximate quantitative agreement: Both studies find that the entry of surface-origin tracers into the tropical stratosphere is strongest over Indonesia, although unlike *Levine et al.* [2007], we do not see a DJF secondary maximum over Africa, which is likely due to the fact that we considered no major African sources, while *Levine et al.* [2007] release their tracers uniformly everywhere between 20°S and 20°N. *Levine et al.* [2007] estimate that 0.5%–1% of a VSLS with $\tau_c = 1$ week, and 3%–4% of a VSLS with $\tau_c = 4$ weeks, have reached the stratosphere within one month. For the roughly corresponding lifetimes of 8 and 21 days, our ocean-source DJF flux ratios are 1.2% and 4.9%, respectively.

[32] The implications of our findings for the importance of bromoform to stratospheric chemistry are therefore also similar to the study of *Levine et al.* [2007]. For any substance of interest with a chemical lifetime τ_c, our flux ratio for that value of τ_c (Figure 2b) can simply be multiplied by the corresponding surface emissions to get a rough estimate of the flow rate with which the substance first enters the stratosphere. Thus, for example, bromoform emissions of 10 Gmol Br/year [*Quack and Wallace*, 2003], with an estimated lifetime roughly bracketed by 8 and 21 days [*Sinnhuber and Folkins*, 2006], imply a flux of 0.12–0.49 Gmol Br/year first entering the stratosphere during DJF (about 25% less in JJA).

[33] Finally, we acknowledge that a more complete study of transport into the stratosphere would not only consider first entry into the stratosphere, but also the residence time within the stratosphere. A detailed analysis of the residence-time-dependent ventilation of the stratosphere from the tropical tropopause has recently been performed by *Orbe et al.* [submitted to JGR-Atmospheres].

References

Aschmann, J., B.-M. Sinnhuber, E. L. Atlas, and S. M. Schauffler (2009), Modeling the transport of very short-lived substances into the tropical upper troposphere and lower stratosphere, *Atmos. Chem. Phys.*, *9*, 9237–9247.

Berthet, G., J. G. Esler, and P. H. Haynes (2007), A Lagrangian perspective of the tropopause and the ventilation of the lowermost stratosphere, *J. Geophys. Res.*, *112*, D18102, doi:10.1029/2006JD008295.

Bonazzola, M., and P. H. Haynes (2004), A trajectory-based study of the tropical tropopause region, *J. Geophys. Res.*, *109*, D20112, doi:10.1029/2003JD004356.

Brioude, J., et al. (2010), Variations in ozone depletion potentials of very short-lived substances with season and emission region, *Geophys. Res. Lett.*, *37*, L19804, doi:10.1029/2010GL044856.

Butler, J. H., et al. (2007), Oceanic distributions and emissions of short-lived halocarbons, *Global Biogeochem. Cycles*, *21*, GB1023, doi:10.1029/2006GB002732.

Decker, M., M. A. Brunke, Z. Wang, K. Sakaguchi, and X. Zeng (2012), Evaluation of the reanalysis products from GSFC, NCEP, and ECMWF using flux tower observations, *J. Climate*, *25*, 1916–1944.

Fueglistaler, S., H. Wernli, and T. Peter (2004), Tropical troposphere-to-stratosphere transport inferred from trajectory calculations, *J. Geophys. Res.*, *109*, D03108, doi:10.1029/2003JD004069.

Gettelman, A., P. H. Lauritzen, M. Park, and J. E. Kay (2009), Processes regulating short-lived species in the tropical tropopause layer, *J. Geophys. Res.*, *114*, D13303, doi:10.1029/2009JD011785.

Gibson, J. K., P. Kallberg, S. Uppala, A. Hernandez, N. A, and E. Serrano (1997), ERA description, *ECMWF Re-Analysis Project Report Series 1*, ECMWF, UK.

Hack, J. J. (1994), Parameterization of moist convection in the NCAR Community Climate Model, CCM2, *J. Geophys. Res.*, *99*, 5551–5568.

Hall, T. M., and M. Holzer (2003), Advective-diffusive mass flux and implications for stratosphere-troposphere exchange, *Geophys. Res. Lett.*, *30*, 1222, doi:10.1029/2002GL016419.

Holzer, M. (1999), Analysis of passive tracer transport as modeled by an atmospheric general circulation model, *J. Climate*, *12*, 1659–1684.

Hossaini, R., M. P. Chipperfield, B. M. Monge-Sanz, N. A. D. Richards, E. Atlas, and D. R Blake (2010), Bromoform and dibromomethane in the tropics: A 3-D model study of chemistry and transport, *Atmos. Chem. Phys.*, *10*, 719–735.

Kerkweg, A., P. Jockel, N. Warwick, S. Gebhardt, C. A. M. Brenninkmeijer, and J. Lelieveld (2008), Consistent simulation of bromine chemistry from the marine boundary layer to the stratosphere Ð Part 2: Bromocarbons, *Atmos. Chem. Phys.*, *8*, 5919–5939.

Kistler, R., et al. (2001), The NCEP/NCAR 50-year reanalysis, *Bull. Amer. Meteor. Soc.*, *82*, 247–267.

Krüger, K., S. Tegtmeier, and M. Rex (2008), Long-term climatology of air mass transport through the Tropical Tropopause Layer (TTL) during NH winter, *Atmos. Chem. Phys.*, *8*, 813–823.

Law, K. S., et al. (2007), Very short-lived halogen and sulfur substances, Chapter 2 in Scientific assessment of ozone depletion: 2006, Global ozone research and monitoring project, *Tech. Rep. 50*, World Meteorological Organization, Geneva, Switzerland.

Levine, J. G., P. Braesicke, N. R. P. Harris, N. H. Savage, and J. A Pyle (2007), Pathways and timescales for troposphere-to-stratosphere transport via the tropical tropopause layer and their relevance for very short lived substances, *J. Geophys. Res.*, *112*, D04308, doi:10.1029/2005JD006940.

Liang, Q., R. S. Stolarski, S. R. Kawa, J. E. Nielsen, A. R. Douglass, J. M. Rodriguez, D. R. Blake, E. L. Atlas, and L. E. Ott (2010), Finding the missing stratospheric Bry: A global modeling study of CHBr3 and CH2Br2, *Atmos. Chem. Phys.*, *10*, 2269–2286.

Logan, J. A., M. J. Prather, S. C. Wofsy, and M. B. McElroy (1978), Atmospheric chemistry: Response to human influence, *Phil. Trans. R. Soc. Lond. A*, *290*, 187–234.

Montzka, S. A., et al. (2011), Ozone-Depleting Substances (ODSs) and related chemicals, Chapter 1 in *Scientific Assessment Of Ozone Depletion: 2010, Global Ozone Research and Monitoring Project*, Tech. Rep. 52, World Meteorological Organization, Geneva, Switzerland.

Olivier, J. G. J., J. A. V. Aardenne, F. Dentener, V. Pagliari, L. N. Ganzeveld, and J. Peters (2005), Recent trends in global greenhouse gas emissions: Regional trends 1970–2000 and spatial distribution of key sources in 2000, *Env. Sc.*, *2*, 81–99.

Orbe, C., M. Holzer, and L. M. Polvani (2012), Flux distributions as robust diagnostics of stratosphere-troposphere exchange, *J. Geophys. Res.*, *117*, D01302, doi:10.1029/2011JD016455.

Palmer, C. J., and C. J. Reason (2009), Relationships of surface bromoform concentrations with mixed layer depth and salinity in the tropical oceans, *Global Biogeochem. Cycles*, *23*, GB2014, doi:10.1029/2008GB003338.

Pawson, S., and M. Fiorino (1998), A comparison of reanalyses in the tropical stratosphere. Part 1: Thermal structure and the annual cycle, *Climate Dynamics*, *14*, 631–644.

Pisso, I., P. H. Haynes, and K. S. Law (2010), Emission location dependent ozone depletion potentials for very short-lived halogenated species, *Atmos. Chem. Phys.*, *10*, 12,025–12,036.

Quack, B., and D. W. R. Wallace (2003), Air-sea flux of bromoform: Controls, rates, and implications, *Global Biogeochem. Cycles*, *17*, 1023, doi:10.1029/2002GB001890.

Rasch, P. J., and M. Lawrence (1998), Recent developments in transport methods at NCAR, in *MPI Workshop on Conservative Transport Schemes*, vol. 265, pp. 65–75, Max-Planck-Institute for Meteorology, Hamburg, Germany.

Rasch, P. J., N. M. Mahowald, and B. E. Eaton (1997), Representations of transport, convection and the hydrologic cycle in chemical transport models: Implications for the modeling of short-lived and soluble species, *J. Geophys. Res.*, *102*, 28,127–28,138.

Sinnhuber, B.-M., and I. Folkins (2006), Estimating the contribution of bromoform to stratospheric bromine and its relation to dehydration in the tropical tropopause layer, *Atmos. Chem. Phys*, *6*, 4755–4761.

Son, S., N. F. Tandon, and L. M. Polvani (2011), The fine-scale structure of the global tropopause derived from COSMIC GPS radio occultation measurements, *J. Geophys. Res.*, *116*, D20113, doi:10.1029/2011JD016030.

Sprenger, M., and H. Wernli (2003), A northern hemispheric climatology of cross-tropopause exchange for the ERA15 time period (1979–1993), *J. Geophys. Res.*, *108*, 8521, doi:10.1029/2002JD002636.

Stohl, A. (2001), A one-year Lagrangian "climatology" of airstreams in the Northern Hemisphere troposphere and lowermost stratosphere, *J. Geophys. Res.*, *106*, 7263–7279.

Tian, W., M. P. Chipperfield, D. S. Stevenson, R. Damoah, S. Dhomse, A. Dudhia, H. Pumphrey, and P. Bernath (2010), Effects of stratosphere-troposphere chemistry coupling on tropospheric ozone, *J. Geophys. Res.*, *115*, D00M04, doi:10.1029/2009JD013515.

Trenberth, K. E., D. P. Stepaniak, and J. M. Caron (2000), The global monsoon as seen through the divergent atmospheric circulation, *J. Climate*, *13*, 3969–3993.

Wohltmann, I., and M. Rex (2008), Improvement of vertical and residual velocities in pressure or hybrid sigma-pressure coordinates in analysis data in the stratosphere, *Atmos. Chem. Phys.*, *8*, 265–272.

World Meteorological Organization (1957), Meteorology—A three-dimensional science. Second session of the commission for aerology, *WMO Bull.*, *4*, 134–138.

Wuebbles, D. J., K. O. Patten, M. T. Johnson, and R. Kotamarthid (2001), New methodology for Ozone Depletion Potentials of short-lived compounds: n-Propyl bromide as an example, *J. Geophys. Res.*, *106*, 14,551–14,571.

Zhang, G. J., and N. A. McFarlane (1995), Sensitivity of climate simulations to the parameterization of cumulus convection in the Canadian Climate Centre general circulation model, *Atmos. Ocean*, *33*, 407–446.